

Electrochemical sensors based on polymer-modified screen-printed graphene electrodes for the detection of pharmaceuticals in aquatic environments

Mineral Processing and Extractive Metallurgy
(Trans. Inst. Min. Metall. B)
1–9

© Institute of Materials, Minerals and Mining
and The AusIMM 2025

Article reuse guidelines:

sagepub.com/journals-permissions

DOI: 10.1177/25726641251384865

journals.sagepub.com/home/mpe



Iva Dimitrievska , Perica Paunović and Anita Grozdanov

Abstract

Detecting contaminants in aquatic environments, including wastewater and natural water bodies, is essential for safeguarding environmental health and ensuring water quality. Pharmaceuticals, often incompletely metabolised by humans and animals, persist in the environment and pose risks to ecosystems due to their bioactivity and accumulation potential. Water, as a vital resource for all industries, including mineral and metallurgy, faces increasing challenges from pollutants, making advanced detection methods crucial. This study investigates the application of polymer-modified screen-printed graphene electrodes for the sensitive detection of doxorubicin. The use of graphene not only in energy storage devices but also in sensors makes such materials important for a green and sustainable economy. Electrode performance was evaluated at three pH levels, within a linear concentration range from 1.5 to 7.4 $\mu\text{mol L}^{-1}$. The electrodes' excellent stability and enhanced sensitivity highlight their potential as cost-effective and rapid tools for monitoring pharmaceutical residues in aquatic environments, contributing to pollution management and environmental protection.

Keywords

Doxorubicin, polyvinylidene fluoride, chitosan, environment, aquatic ecosystems, graphene sensors, sustainable economy

Received: 1 July 2025; accepted: 16 September 2025

Introduction

Electrochemical sensors based on screen-printed electrodes (SPEs) have emerged as powerful analytical tools for real-time monitoring of pharmaceutical compounds. These sensors offer significant advantages for practical applications, including rapid response time, minimal sample preparation, cost-effective instrumentation, and the ability to perform measurements in complex matrices using small sample volumes (20–100 μL). The single-use nature of SPEs eliminates cross-contamination concerns, making them ideal for clinical environments.¹

Surface modification of SPEs with nanomaterials has revolutionised their sensing capabilities. Carbon nanomaterials such as graphene and carbon nanotubes significantly enhance electrode sensitivity by increasing the electroactive surface area and accelerating electron transfer rates. Additionally, polymer modifications with chitosan (Ch) and polyvinylidene fluoride (PVDF) further improve sensor performance through interaction mechanisms that promote analyte adsorption and specificity.

These advanced electrochemical platforms have proven particularly valuable for monitoring doxorubicin hydrochloride (DOX), a widely used anticancer medication effective against numerous malignancies. Despite its efficacy, the treatment with DOX is associated with high risks,² such as dose-dependent cardiotoxicity that can cause irreversible heart damage.³ Moreover, DOX has a short half-life in the blood, and

about half is excreted. The biodegradability of DOX as a pollutant from wastewater can be difficult and might have long-lasting negative effects. Graphene-based sensors for pharmaceutical pollutants in water are therefore gaining significant attention. Water is an important resource for all industries, including mineral and metallurgy, which utilise vast quantities for processes such as flotation, hydrometallurgy, and dust control, but also generate substantial wastewater streams often laden with complex contaminants. The presence of pharmaceutical residues, even at trace levels, in these industrial effluents and subsequently in natural water bodies, poses a considerable threat to aquatic ecosystems and human health via the food chain. Therefore, developing a method for sensitive detection and remediation is crucial. The unique properties of graphene, such as its large surface area, excellent electrical conductivity, and ease of functionalisation, make it an ideal candidate for developing next-generation sensors. Also, the

Organic Technology Institute, Faculty of Technology and Metallurgy, Ss. Cyril and Methodius University in Skopje, Skopje, Republic of North Macedonia

Corresponding author:

Iva Dimitrievska, Organic Technology Institute, Faculty of Technology and Metallurgy, Ss. Cyril and Methodius University in Skopje, Rudjer Bošković 16, 1000 Skopje, Republic of North Macedonia.

Email: iva@tmf.ukim.edu.mk

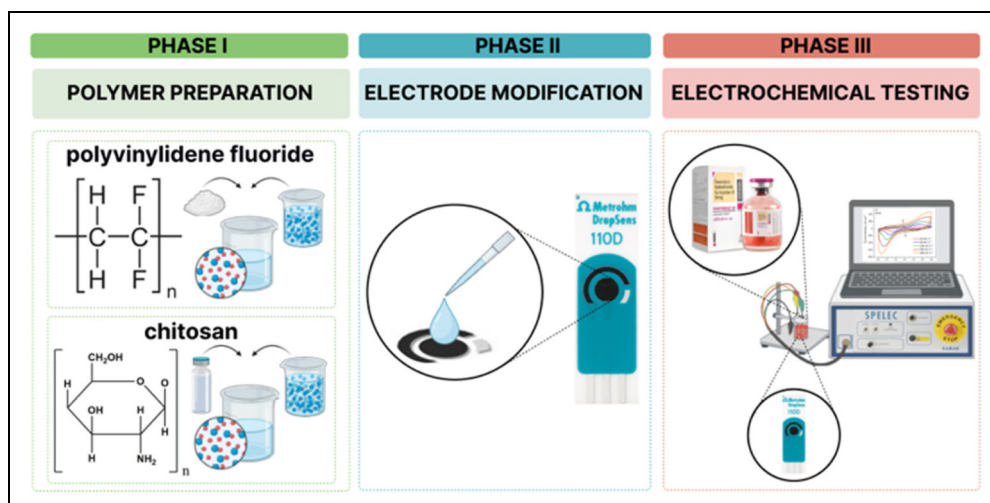


Figure 1. Schematic diagram of the electrodes' preparation, modification, and electrochemical testing.

use of graphene not only in energy storage devices but also in sensors makes them important for greening and a sustainable economy. By enabling rapid, on-site, and cost-effective detection of pharmaceutical pollutants, graphene-based sensors can play a vital role in environmental monitoring, facilitating timely intervention and supporting sustainable water management practices within various industrial sectors and municipal wastewater treatment. This, in turn, contributes to the broader goals of environmental protection and the transition towards a circular and sustainable economy.

Conventional analytical methods for DOX determination include high-performance liquid chromatography and mass spectroscopy techniques that require complex sample preparation and expensive equipment, making electrochemical sensors an attractive alternative for wastewater monitoring. The continued development of these sensing platforms promises to deliver accessible field-deployable devices for environmental monitoring, ultimately improving water quality assessment through rapid detection of pharmaceutical contaminants in wastewater treatment facilities and natural water bodies. In our work, we propose a simple development of an electrochemical sensor based on the SPEs for the detection of doxorubicin (DOX) in aquatic media, aiming to contribute to these advanced monitoring solutions.

Experimental

For this study, two distinct types of modified sensors were prepared using graphene-based SPEs (model DS1100, Dropsens Ltd, Spain) as substrates. The process involved modifying two separate sets of SPEs. The first set was modified with Ch, while the second set was separately modified with PVDF. Both polymer solutions (Sigma Aldrich) were prepared as 2 wt-% solutions in N,N-dimethylacetamide. The modification was performed by drop-casting the respective polymer solution onto the surface of the electrodes, which were then allowed to dry at room temperature. This procedure resulted in two distinct groups of sensors for investigation: one set modified with Ch (G/Ch) and another with PVDF (G/PVDF). The schematic diagram of this process is shown in Figure 1.

Electrochemical measurements

All electrochemical measurements were conducted at 25 °C in 25 mL 0.1 mol L⁻¹ phosphate buffer saline (PBS), at pH 6.7. The influence of pH was initially screened at pH 4.0 and 11.0 to establish optimal electrolyte conditions. Doxorubicin stock solution (DOX, Ebewe a.d., 2 mg mL⁻¹) was added to the electrolyte to a concentration of 0.002 mol L⁻¹.

Cyclic voltammetry (CV) was employed for the electrochemical characterisation using a SPELEC potentiostat controlled by Dropview software. Voltammetric scans were performed within a potential window of -0.05 to +0.6 V for five cycles. A scan rate of 50 mV/s was selected as optimal for balancing the sensitivity and stability of the DOX redox signals. A calibration curve was constructed in the concentration range of 1.5–7.4 μmol L⁻¹ to establish the analytical performance of the sensors. All measurements were performed in triplicate.

Electrochemical data analysis and characterisation

The analytical performance of each sensor was evaluated from the parameters of its corresponding calibration curve. The limit of detection (LOD) and limit of quantification (LOQ) were calculated based on the standard deviation of the response and the slope of the calibration curve, using the following equations:

$$\text{LOD} = \frac{(3 * \sigma)}{S}, \quad (1)$$

$$\text{LOD} = \frac{(10 * \sigma)}{S}, \quad (2)$$

where S represents the slope of the calibration curve (sensitivity), and σ is the standard deviation of the response, typically estimated from the standard deviation of the y -intercept of the regression line. This approach provides a statistical estimation of the lowest analyte concentration that can be reliably detected and quantified, respectively.

To gain a deeper insight into the electron transfer kinetics of DOX at the electrode surface, the heterogeneous rate constant (k^0) was calculated using the method proposed by Nicholson.^{4,5} For a quasi-reversible process, this method involves two steps.

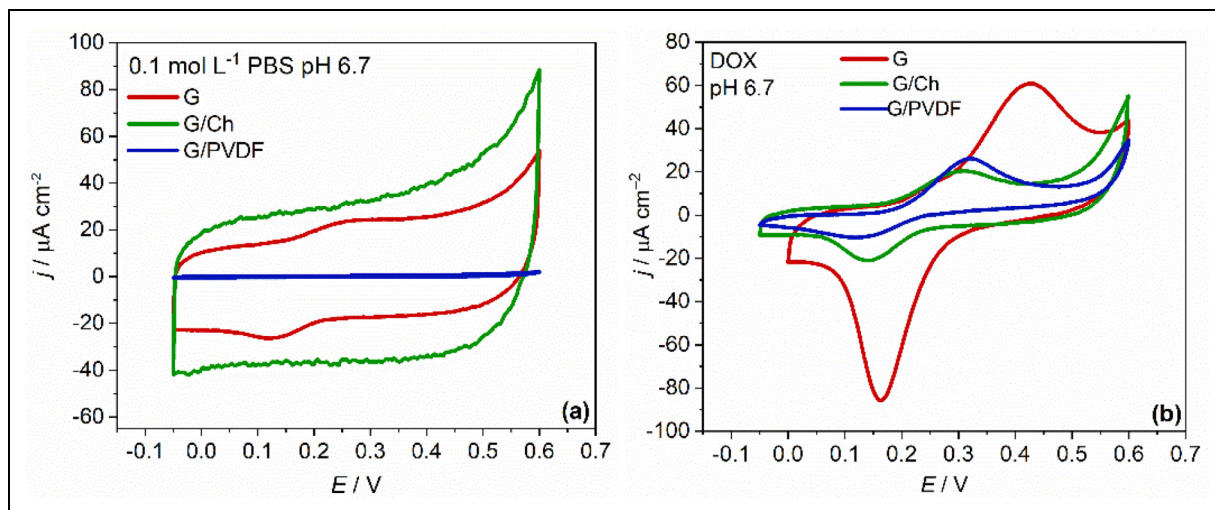


Figure 2. SPEs' response in (a) 0.1 mol L⁻¹ PBS and (b) 0.002 mol L⁻¹ DOX solution at pH 6.7. SPE: screen-printed electrode; PBS: phosphate buffer saline; DOX: doxorubicin hydrochloride.

First, the dimensionless kinetic parameter Ψ is estimated from the experimentally determined peak separation (ΔE_p) using the empirical equation (3) developed by Swaddle⁵:

$$\ln\Psi = 3.69 - 1.16 \ln(\Delta E_p[\text{mV}] - 59), \quad (3)$$

where ΔE_p is the difference between the anodic and cathodic peak potentials in millivolts. Subsequently, the heterogeneous rate constant (k^0) is calculated from Ψ using the following equation:

$$\Psi = \frac{k^0}{\left[\pi D\nu \left(\frac{F}{RT}\right)\right]^{\frac{1}{2}}} \gamma^{\frac{\alpha}{2}}, \quad (4)$$

where D is the diffusion coefficient of DOX (using a literature value of $3.4 \times 10^{-6} \text{ cm}^2 \text{ s}^{-1}$)⁶, ν is the scan rate (V s^{-1}), γ is the ratio of diffusion coefficients (assumed to be 1), α is the charge transfer coefficient, and F is the Faraday constant ($96,485 \text{ C mol}^{-1}$), R is the universal gas constant ($8.314 \text{ J mol}^{-1} \text{ K}^{-1}$), and T is the absolute temperature in Kelvin (298.15 K for measurements conducted at $25 \text{ }^\circ\text{C}$).

The electrochemically active surface area (EASA) of the electrodes was estimated by determining the electrochemical double-layer capacitance (C_{dl}). This was achieved by recording cyclic voltammograms at various scan rates (ν) in a potential region where no Faradaic processes occur. The capacitive current (I_{cap}) was determined at a specific potential within this region according to the following equation:

$$I_{cap} = \frac{|I_{p,a}| + |I_{p,c}|}{2}, \quad (5)$$

where $I_{p,a}$ and $I_{p,c}$ are the anodic and cathodic currents, respectively. The value of C_{dl} was then determined from the slope of the linear plot of I_{cap} versus the scan rate (ν).

Finally, the EASA was calculated using the following relationship:

$$EASA = \frac{C_{dl}A}{C_s^*}, \quad (6)$$

where A is the geometric area of the electrode (0.12566 cm^2), and C_s^* is the specific capacitance of an ideally smooth

surface of a similar material. A standard value of $25 \mu\text{F cm}^{-2}$ for a smooth carbon-based surface was used as a reference for this calculation.⁷

The analytical performance and reliability of the sensors were validated by assessing their repeatability, intermediate precision, and long-term stability. Repeatability (also known as intra-day precision) was determined by conducting ten consecutive CV measurements using a single modified electrode in a solution of 0.002 mol L^{-1} DOX in 0.1 mol L^{-1} PBS. The relative standard deviation (RSD) of the resulting peak currents was calculated to quantify the repeatability.

Intermediate precision (or inter-electrode precision) was evaluated to assess the consistency between different sensors. For this, three separate, freshly modified electrodes of each type were prepared, and a CV measurement was performed with each in the same DOX solution. The RSD of the peak currents from the three electrodes was then calculated.

The long-term stability of the sensor was evaluated over seven days. An initial measurement was recorded in a 0.002 mol L^{-1} DOX solution, which served as the day 1 response. The electrode was then gently rinsed with deionised water, allowed to dry, and stored under ambient laboratory conditions. On the seventh day, the same electrode was retested in a freshly prepared DOX solution of the same concentration. The stability was determined by comparing the peak current response from day 7 to the initial response recorded on day 1, with the result expressed as a percentage of signal retention.

Results and discussions

Three electrode systems based on commercial graphene (G), Ch-modified graphene (G/Ch), and PVDF-modified graphene (G/PVDF), were evaluated by CV in 0.1 mol/L PBS with and without DOX, at three different pH values (4.0, 6.7, and 11.0). The voltammograms were recorded in a potential range of -0.05 – 0.6 V at a scan rate of 50 mV s^{-1} .

In PBS alone (Figures 2(a), 3(a) and 4(a)), all electrodes showed minimal background current with no redox peaks, confirming a stable baseline for measurements. This absence

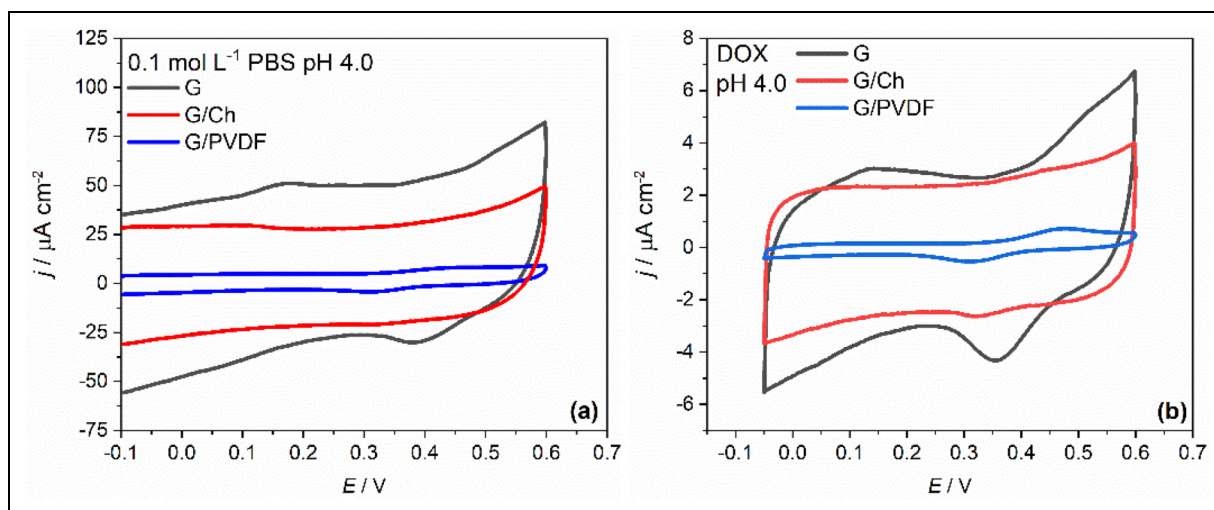


Figure 3. SPEs' response in (a) 0.1 mol L⁻¹ PBS and (b) 0.002 mol L⁻¹ DOX solution at pH 4.0. SPE: screen-printed electrode; PBS: phosphate buffer saline; DOX: doxorubicin hydrochloride.

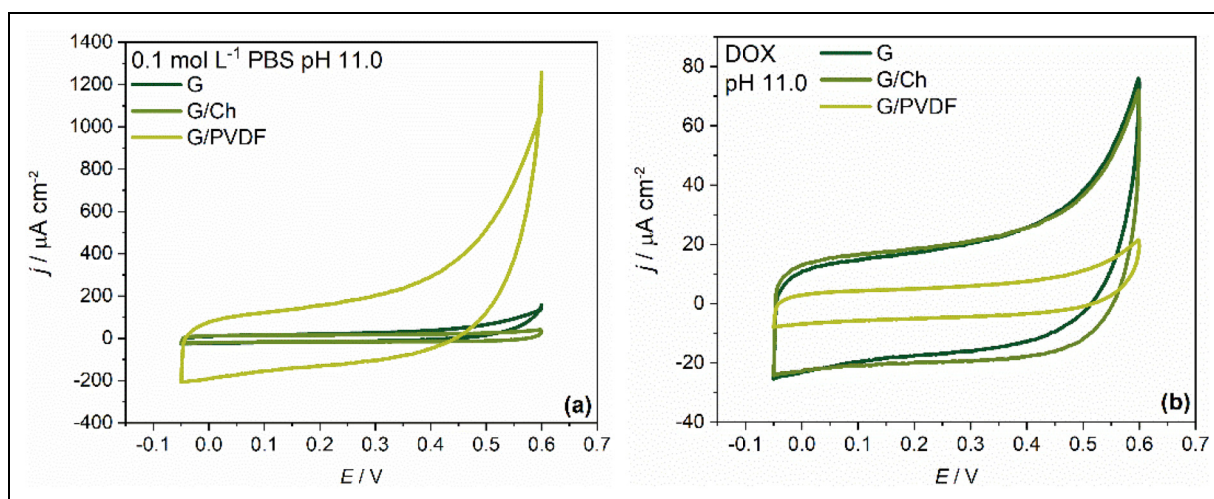


Figure 4. SPEs' response in (a) 0.1 mol L⁻¹ PBS and (b) 0.002 mol L⁻¹ DOX solution at pH 11.0. SPE: screen-printed electrode; PBS: phosphate buffer saline; DOX: doxorubicin hydrochloride.

of peaks indicates that the electrolyte solution does not contain electroactive species under the experimental conditions, ensuring a clear distinction between background response and signals from added analytes.

Upon addition of DOX (0.002 mol L⁻¹) at pH 6.7, all electrodes displayed characteristic oxidation (P_{ox}) and reduction (P_{red}) peaks. A visual inspection reveals key performance differences: the commercial graphene electrode (G) exhibited the strongest current response, but with a broader peak-to-peak separation potential (ΔE_p). In contrast, the polymer-modified electrodes, particularly G/Ch, demonstrated more favourable electron transfer kinetics, evidenced by a significantly smaller ΔE_p . These improvements result from specific interactions between DOX and the polymers, including π - π stacking, hydrogen bonding, and hydrophobic interactions.⁸⁻¹⁰ The electrochemical parameters for all SPEs at pH 4.0 and 6.7 are given in Table 1, while all general observations are quantified and analysed in detail below.

A detailed analysis of the parameters in Table 1 provides a comprehensive understanding of the electrode performances at neutral pH. For an ideal, fully reversible

electrochemical process involving one electron, the theoretical ΔE_p is approximately 59/ n mV (where n is the number of electrons), and the peak current ratio (I_{ox}/I_{red}) is equal to 1.¹¹⁻¹⁴ While the complex electrochemistry of DOX rarely meets these ideal criteria, these theoretical values serve as excellent criteria for comparing the relative performance and kinetic favourability of different electrode systems.

The reversibility of the redox reaction was evaluated against these criteria. Compared to the commercial graphene electrode (G), which exhibited a large ΔE_p of 166 mV, both polymer-modified electrodes showed significantly improved kinetics. The G/Ch electrode demonstrated the best performance, with a ΔE_p of only 129 mV. Although this value is higher than the theoretical limit for a fully reversible process, this substantial reduction indicates a more facile and kinetically favourable electron transfer process compared to the bare electrode.

This enhanced reversibility is further confirmed by I_{ox}/I_{red} . The G/Ch electrode displayed a ratio of 1.001, which is nearly ideal and signifies a highly stable redox couple

Table 1. Electrochemical parameters calculated for all graphene electrodes.

Electrode	P_{ox} (mV)	P_{red} (mV)	ΔE_p (mV)	$E_{1/2}$	I_{ox} (μA)	I_{red} (μA)	I_{ox}/I_{red}
pH 4.0							
G	427	164	263	295.5	3.407	-4.321	0.788
G/chitosan	310	142	167	226	3.013	-2.641	1.141
G/PVDF	322	196	195	259	0.742	-0.569	1.305
pH 6.7							
G	523	357	166	318	7.710	-10.723	0.719
G/chitosan	451	322	129	226	2.648	-2.646	1.001
G/PVDF	473	312	161	258.5	3.467	-1.340	2.587

G: graphene; G/PVDF: polyvinylidene fluoride-modified graphene.

Table 2. Calculated surface and kinetic parameters for the graphene electrodes at pH 6.7.

Electrode	C_{dl} ($\mu F cm^{-2}$)	EASA (cm^2)	α (for $n=2$)	k^0 ($cm s^{-1}$)
G	384	1.93	0.88	1.71×10^{-5}
G/chitosan	338	1.70	0.89	3.54×10^{-5}
G/PVDF	46	0.23	0.86	2.74×10^{-5}

EASA: electrochemically active surface area; G: graphene; G/PVDF: polyvinylidene fluoride-modified graphene.

with minimal loss of electroactive species between scans. This indicates that the process on the G/Ch surface is highly quasi-reversible. In contrast, the G/PVDF electrode showed a much higher ratio of 2.587, and the bare graphene electrode a ratio of 0.719, both deviating significantly from the ideal value, which points to more complex or less stable reaction mechanisms on their respective surfaces.

These findings indicate that the polymer modifications, particularly with chitosan, facilitate a faster and more reversible electron exchange, resulting in a highly quasi-reversible system. While the G/PVDF modification also improves the peak separation compared to bare graphene, its poor current ratio suggests a less stable or more complex reaction mechanism on its surface. Therefore, the G/Ch electrode is identified as the superior candidate at neutral pH.

To provide a deeper, quantitative insight into the fundamental reasons for these performance differences, the EASA and the heterogeneous electron transfer rate constant (k^0) were calculated for each system. These parameters allow for the deconvolution of the contributions from the physical surface area and the intrinsic catalytic activity of the electrode modifications.

The calculated parameters, summarised in Table 2, demonstrate the complex relationship between the surface area and catalytic activity of the electrodes. The bare graphene electrode exhibits an exceptionally high C_{dl} value of $384 \mu F cm^{-2}$, corresponding to a large EASA of $1.93 cm^2$. On the contrary, the G/PVDF electrode exhibits a dramatic decrease in C_{dl} to only $46 \mu F cm^{-2}$, resulting in a reduction of the EASA by nearly 90%. This quantitatively confirms that the PVDF layer acts as a passivating film, physically blocking a significant portion of the active surface. The G/Ch electrode, however, shows only a minor decrease in C_{dl} ($338 \mu F cm^{-2}$), indicating the formation of a thin, conformal polymer layer that preserves most of the underlying active surface.

More importantly, the kinetic analysis reveals the superior catalytic properties of the modified surfaces. The G/Ch

electrode exhibited the highest heterogeneous rate constant ($k^0 = 3.54 \times 10^{-5} cm s^{-1}$), a value more than twice as high as that of the unmodified graphene electrode ($1.71 \times 10^{-5} cm s^{-1}$). This is a crucial finding, as it provides direct evidence that the Ch film is not merely a passive layer but an active catalyst that significantly accelerates the rate of electron transfer. The G/PVDF electrode also shows an enhanced rate constant ($k^0 = 2.74 \times 10^{-5} cm s^{-1}$) compared to the bare graphene.

These results demonstrate that the superior overall performance of the G/Ch electrode can be attributed to an optimal combination of a large, well-preserved active surface area and the highest intrinsic catalytic activity, which results in both a high current response and fast, quasi-reversible kinetics. Contrary to this, while the G/PVDF modification also enhances the reaction rate, its analytical performance is ultimately limited by the drastic reduction in the available active surface area.

In an acidic environment (pH 4.0), all electrodes exhibited a notable shift in the position and intensity of redox peaks compared to neutral conditions (Figure 3(b) and Table 1). The commercial graphene electrode showed a decrease in P_{ox} with reduced peak current intensity. While literature suggests that mildly acidic media (pH 4.5–5.5) are favourable for DOX detection,^{15–17} a more strongly acidic pH environment (4.0) proved detrimental to its performance.

Both polymer-modified electrodes demonstrated superior performance relative to the bare graphene at this pH. The G/Ch electrode exhibited the most enhanced characteristics, with a significantly smaller ΔE_p (167 mV) and an improved I_{ox}/I_{red} of 1.141, which can be attributed to the protonation of amino groups in chitosan at acidic pH.¹⁸ This creates additional positively charged sites that can electrostatically attract the doxorubicin molecule, leading to more favourable interaction and improved electrochemical response even under otherwise detrimental pH conditions.

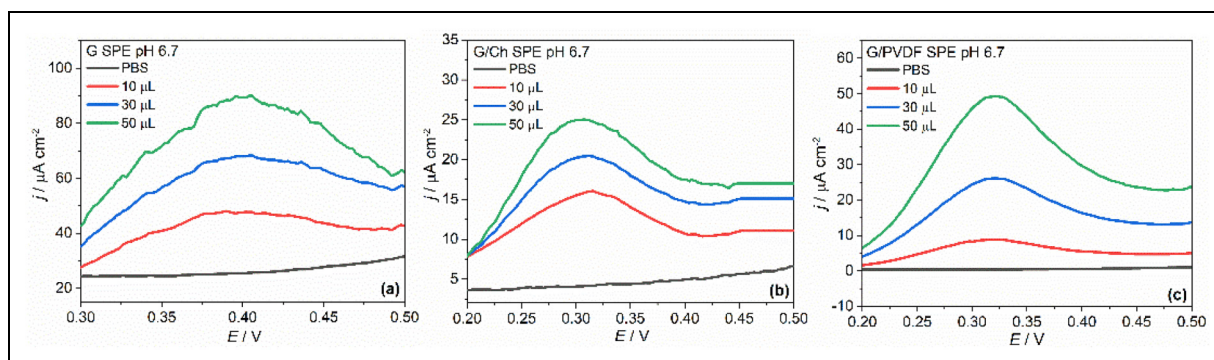


Figure 5. Cyclic voltammograms of (a) G, (b) G/Ch, and (c) G/PVDF electrodes in 0.1 mol L^{-1} PBS (pH 6.7) with increasing concentrations of DOX.

G: graphene; Ch: chitosan; G/Ch: Ch-modified graphene; G/PVDF: polyvinylidene fluoride-modified graphene; PBS: phosphate buffer saline; DOX: doxorubicin hydrochloride.

At a highly alkaline pH of 11.0, as shown in Figure 4(b), the characteristic redox peaks for DOX completely disappeared on all three electrode systems.

The electrochemical observation was accompanied by a distinct visual change in the electrolyte solution, which transitioned from its typical red colour to a deep violet. A change in the colour is a clear indicator of the irreversible chemical degradation of the doxorubicin molecule via hydrolysis, a process known to occur rapidly under strongly alkaline conditions.^{19–21} This finding is important because it demonstrates that the absence of a signal is not due to a failure of the sensor, but rather that the sensor is correctly reporting the absence of the electroactive analyte in its original form. This result defines the upper operational limit of the analytical method and confirms that the detection of DOX is not feasible in highly alkaline environments due to the inherent instability of the drug molecule itself.

These pH-dependent responses demonstrate the versatility of polymer-modified electrodes across different chemical environments, with G/Ch and G/PVDF performing optimally in neutral to slightly acidic conditions. The consistent improvement in electrochemical parameters compared to unmodified graphene electrodes confirms that strategic polymer modification creates more favourable environments for DOX detection through the combined effects of increased surface area, enhanced conductivity, and specific chemical interactions.

To further evaluate and quantify the analytical performance under different conditions, calibration studies were performed. The electrochemical response of each electrode was monitored with successive additions of DOX at both neutral (pH 6.7) and acidic (pH 4.0) environments. The resulting series of voltammograms recorded at the optimal neutral pH are presented in Figure 5.

As is visually evident, the anodic peak current increases proportionally with the DOX concentration for all three systems. From these voltammograms, calibration curves were constructed within a linear concentration range of $1.5\text{--}7.4 \text{ } \mu\text{mol L}^{-1}$, as displayed in Figure 6.

The G/Ch electrode (Figure 6(b)) demonstrated the highest correlation coefficient ($R^2 = 0.9937$). The G/PVDF system (Figure 6(c)) followed with $R^2 = 0.9843$, while the unmodified graphene electrode (Figure 6(a)) showed a correlation of $R^2 = 0.9696$. Sensitivity values were determined to be 0.088 , 0.150 , and $0.274 \text{ } \mu\text{A } \mu\text{mol}^{-1} \text{ L}$ for G/Ch, G/

PVDF, and G systems, respectively. Both modified electrodes achieved lower LOD and LOQ compared to the unmodified electrode. The G/Ch system performed best with LOD and LOQ values of 9.822 and $32.741 \text{ } \mu\text{mol L}^{-1}$, respectively, followed closely by G/PVDF with values of 9.869 and $32.896 \text{ } \mu\text{mol L}^{-1}$. The commercial graphene electrode showed the highest limits at 9.943 and $33.144 \text{ } \mu\text{mol L}^{-1}$ for LOD and LOQ, respectively.

The quantitative analysis of the electrodes was also performed in an acidic environment (PBS at pH 4.0). The series of voltammograms recorded at pH 4.0 are shown in Figure 7. Under these conditions, the correlation coefficients (R^2) for the calibration curves were notably lower compared to those obtained at neutral pH, indicating a less consistent electrochemical response. Specifically, the unmodified graphene electrode (G) exhibited a sensitivity of $0.548 \text{ } \mu\text{A } \mu\text{mol}^{-1} \text{ L}$ with a correlation coefficient (R^2) of 0.72 . The G/Ch showed a sensitivity of $0.265 \text{ } \mu\text{A } \mu\text{mol}^{-1} \text{ L}$ ($R^2 = 0.78$), while the G/PVDF had the lowest sensitivity of $0.084 \text{ } \mu\text{A } \mu\text{mol}^{-1} \text{ L}$, with the highest correlation coefficient of the group ($R^2 = 0.89$).

Consistent with the decrease in signal reproducibility, the LOD and LOQ increased for all systems in the acidic medium. The G electrode had an LOD of $11.52 \text{ } \mu\text{mol L}^{-1}$ and an LOQ of $38.41 \text{ } \mu\text{mol L}^{-1}$. The G/Ch electrode showed an LOD of $11.08 \text{ } \mu\text{mol L}^{-1}$ and an LOQ of $36.92 \text{ } \mu\text{mol L}^{-1}$. Notably, the G/PVDF electrode, despite its lower sensitivity, possessed the most favourable LOD ($10.35 \text{ } \mu\text{mol L}^{-1}$) and LOQ ($34.51 \text{ } \mu\text{mol L}^{-1}$) in the acidic environment, suggesting good stability of the polymer film. Overall, these results indicate that while DOX remains electrochemically active at low pH, the signal sensitivity and reproducibility are significantly diminished, likely due to altered protonation states of the analyte or unfavourable interactions with the electrode surface.

The obtained results highlight the improved electrochemical performance of the polymer-modified electrodes, particularly the chitosan modification, which demonstrated superior sensitivity and analytical performance for DOX detection in neutral media.

Repeatability, stability, and reproducibility

The repeatability, stability, and reproducibility of the commercial and modified SPEs were evaluated using CV in a

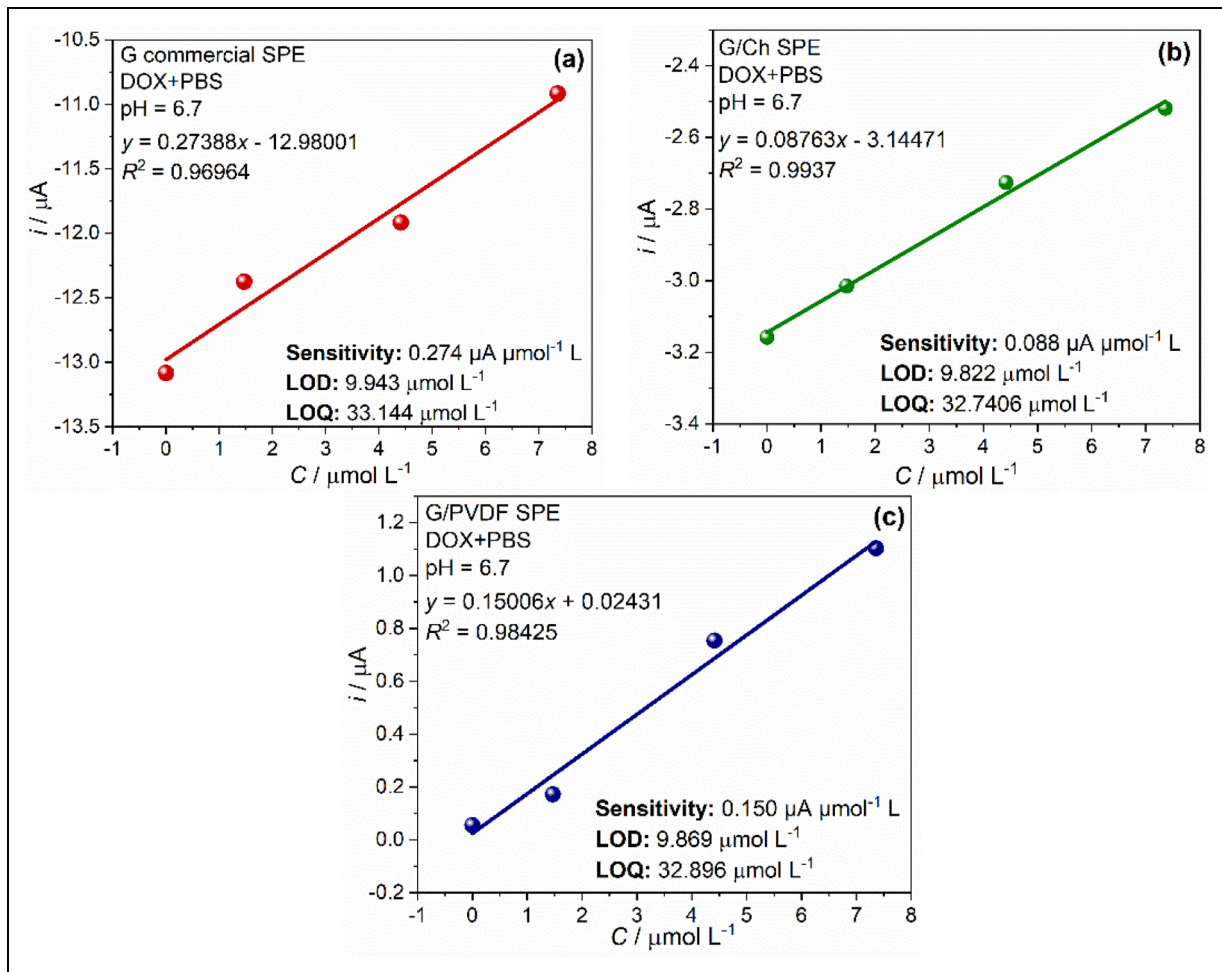


Figure 6. Current (I)–concentration (C) at pH 6.7 for (a) G, (b) G/Ch, and (c) G/PVDF. G: graphene; Ch: chitosan; G/Ch: Ch-modified graphene; G/PVDF: polyvinylidene fluoride-modified graphene.

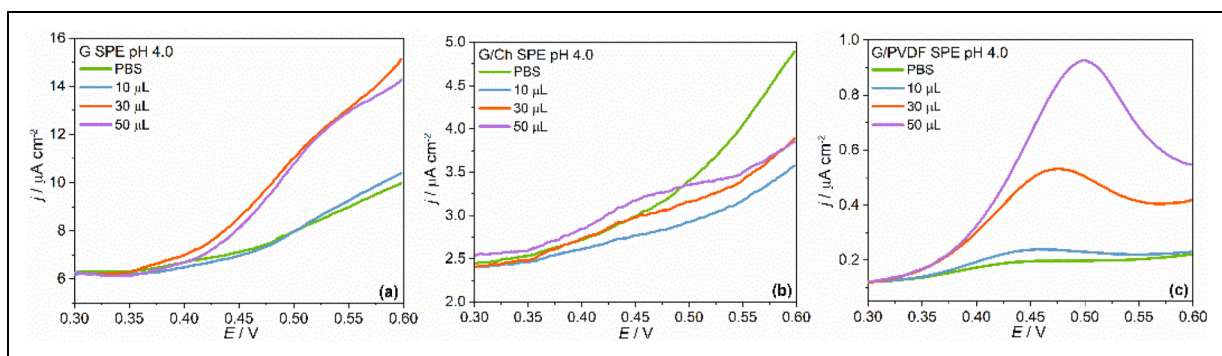


Figure 7. Cyclic voltammograms of (a) G, (b) G/Ch, and (c) G/PVDF electrodes in 0.1 mol L^{-1} PBS (pH 4.0) with increasing concentrations of DOX. G: graphene; Ch: chitosan; G/Ch: Ch-modified graphene; G/PVDF: polyvinylidene fluoride-modified graphene; PBS: phosphate buffer saline; DOX: doxorubicin hydrochloride.

0.002 mol L^{-1} DOX solution prepared in 0.1 mol L^{-1} PBS at pH 6.7.

Repeatability was assessed from 10 consecutive measurements, yielding low RSD values of 4.47% for the commercial graphene (G), 1.76% for the G/Ch, and 3.43% for the G/PVDF electrode.

The long-term stability of the sensors was monitored over 7 days. The G/Ch electrode demonstrated excellent stability, with its oxidation peak current decreasing by only 4.95%

from the initial value. The G/PVDF and commercial G electrodes showed slightly higher, yet still acceptable, current losses of 12.45% and 12.88%, respectively. The high stability of the G/Ch sensor is visually demonstrated in Figure 8, which overlays the first and tenth CV cycles from Day 1 and Day 7. The minimal change between the voltammogram on Day 1 (solid blue line) and Day 7 (solid pink line) provides clear visual confirmation of the sensor's robust long-term performance. Additionally, the near-identical overlap

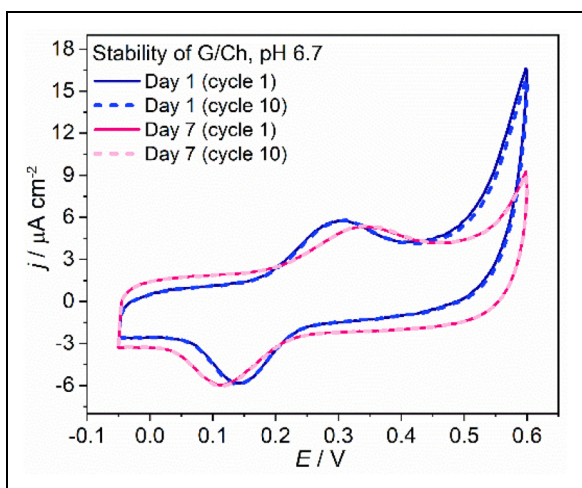


Figure 8. Stability of G/Ch electrode in 0.002 mol L^{-1} DOX solution (pH 6.7) over seven days. G: graphene; Ch: chitosan; G/Ch: Ch-modified graphene; DOX: doxorubicin hydrochloride.

between the first and tenth cycles on each respective day highlights the sensor's excellent operational stability.


Finally, the inter-electrode reproducibility was evaluated using three different, newly prepared sensors for each modification. The analysis yielded low RSD values of 3.05% (G), 3.48% (G/Ch), and 3.04% (G/PVDF), demonstrating the excellent consistency and reliability of the sensor fabrication method.

Conclusions

This research successfully developed polymer-modified screen-printed graphene electrodes for sensitive electrochemical detection of doxorubicin in aquatic media. The modified electrodes, particularly the G/Ch electrode, exhibited superior performance compared to a commercial, unmodified electrode. The electrochemical response was significantly influenced by pH, with optimal performance observed at neutral pH (6.7). At this pH, the G/Ch electrode demonstrated excellent analytical parameters, including the lowest limits of detection and quantification and the highest linearity. The study provides a fundamental explanation for these enhanced performances. Both polymer modifications improved electron transfer kinetics, evidenced by a significantly reduced peak-to-peak separation potential. A detailed analysis revealed that the superior performance of the G/Ch electrode is attributed to an optimal synergy between a large, well-preserved EASA and the highest intrinsic catalytic activity, as confirmed by its calculated heterogeneous rate constant (k^0), which was more than twice that of the bare graphene. The exceptional repeatability, stability, and reproducibility of the G/Ch electrode further highlight its potential for practical applications. These findings demonstrate that polymer-modified screen-printed electrodes represent a promising platform for the development of cost-effective, portable, and reliable sensors for monitoring pharmaceutical contaminants in environmental water samples. Their implementation could significantly contribute to monitoring efforts in wastewater treatment facilities and natural water bodies, providing a valuable tool for

environmental protection and water quality assessment, and supporting the broader objectives of a sustainable, green economy.

ORCID iD

Iva Dimitrievska  <https://orcid.org/0000-0002-7196-1875>

Funding

The authors received no financial support for the research, authorship, and/or publication of this article.

Declaration of conflicting interests

The authors declared no potential conflicts of interest with respect to the research, authorship, and/or publication of this article.

References

- Dimitrievska I, Paunović P and Grozdanov A. Polymer-modified screen-printed electrode-based electrochemical sensors for doxorubicin detection. *J Electrochem Sci Eng* 2024; 15: 2501.
- Jinga LI, Tudose M and Ionita P. Laccase-TEMPO as an efficient system for doxorubicin removal from wastewaters. *Int J Environ Res Public Health* 2022; 19: 6645.
- Mitry MA and Edwards JG. Doxorubicin induced heart failure: phenotype and molecular mechanisms. *Int J Cardiol Heart Vasculature* 2016; 10: 17–24.
- Nicholson RS. Theory and application of cyclic voltammetry for measurement of electrode reaction kinetics. *Anal Chem* 1965; 37: 1351–1355.
- Swaddle TW. Homogeneous versus heterogeneous self-exchange electron transfer reactions of metal complexes: insights from pressure effects. *Chem Rev* 2005; 105: 2573–2608.
- Tajik S, Beitollahi H, Garkani Nejad F, et al. Electrochemical determination of doxorubicin in the presence of dacarbazine using MWCNTs/ZnO nanocomposite modified disposable screen-printed electrode. *Biosensors* 2025; 15: 60.
- Marsan B, Fradette N and Beaudoin G. Physicochemical and electrochemical properties of CuCO_2O_4 electrodes prepared by thermal decomposition for oxygen evolution. *J Electrochem Soc* 1992; 139: 1889–1896. <https://doi.org/10.1149/1.2069516>
- Chekin F, Myshin V, Ye R, et al. Graphene-modified electrodes for sensing doxorubicin hydrochloride in human plasma. *Anal Bioanal Chem* 2019; 411: 1509–1516.
- Imran H, Tang Y, Wang S, et al. Optimized DOX drug deliveries via chitosan-mediated nanoparticles and stimuli responses in cancer chemotherapy: a review. *Molecules* 2024; 29: 31.
- Apetrei IM and Apetrei C. Voltametric determination of melatonin using a graphene-based sensor in pharmaceutical products. *Int J Nanomed* 2016; 11: 1859–1866.
- Kokoshkarova P. PhD thesis, Faculty of Natural Sciences, Ss. Cyril and Methodius University in Skopje, North Macedonia, <https://eprints.ugd.edu.mk/id/eprint/35744> (2023).
- Bard AJ and Faulkner LR. *Electrochemical methods. Fundamentals and applications*. 3rd edition. New York, NY, USA: John Wiley & Sons, Inc, 2004, ISBN: 978-1-119-33405-7.
- Evans DH, O'Connell KM, Petersen RA, et al. Cyclic voltammetry. *J Chem Educ* 1983; 60: 90.

14. Bott AW. Characterization of chemical reactions coupled to electron transfer reactions using cyclic voltammetry. *Curr Sep* 1999; 18: 9. <http://www.currentseparations.com/issues/18-1/cs18-1b.pdf>
15. Materon EM, Wong A, Filho OF, et al. Development of a simple electrochemical sensor for the simultaneous detection of anticancer drugs. *J Electroanal Chem* 2018; 827: 64–72.
16. Mahdavi M, Rahmani F and Nouranian S. Molecular simulation of pH-dependent diffusion, loading, and release of doxorubicin in graphene and graphene oxide drug delivery systems. *J Mater Chem B* 2016; 1: 7441–7451.
17. Rungnim C, Rungrotmongkol T and P R. Pooarporn, pH-controlled doxorubicin anticancer loading and release from carbon nanotube noncovalently modified by chitosan: MD simulations. *J Mol Graphics Modell* 2016; 70: 70–76.
18. Li J, et al. Molecular dynamics study on the encapsulation and release of anti-cancer drug doxorubicin by chitosan. *Int J Pharm* 2020; 580: 119241.
19. Kaushik D and Bansal G. Four new degradation products of doxorubicin: an application of forced degradation study and hyphenated chromatographic techniques. *J Pharm Anal* 2015; 5: 285–295.
20. Mosafra J and Teymouri M. Comparative study of superparamagnetic iron oxide/doxorubicin co-loaded poly (lactic-co-glycolic acid) nanospheres prepared by different emulsion solvent evaporation methods. *Artif Cells Nanomed Biotechnol* 2017; 46: 1146–1155.
21. Szota M and Jachimska B. Effect of alkaline conditions on forming an effective G4.0 PAMAM complex with doxorubicin. *Pharmaceutics* 2023; 15: 75.